DOI: 10.31401/WS.2025.proc.14

The Geomagnetic Midlatitude Effects of the Supersubstorms during May 10-12, 2024 Superstorm

Guineva V.H.[1], Despirak I.V.[2], Werner R.[1], Lubchich A.A.[2], Raykova L.[1], Bojilova R.[3]

[1]Space Research and Technology Institute (SRTI), Bulgarian Academy of Sciences, Stara Zagora Department, Bulgaria
v_guineva@yahoo.com
[2]Polar Geophysical Institute (PGI), Apatity, Russia
[3]National Institute of Geophysics, Geodesy and Geography (NIGGG) - Bulgarian Academy of Sciences, Sofia, Bulgaria

Abstract

The aim of this study is to conduct the detailed analysis of the geomagnetic auroral and midlatitude disturbances during the superstorm on 10–12 May 2024. It was the second-strongest geomagnetic storm of the space era (SYM/H ~ -518 nT). Storm main phase was observed from ~17:15 UT on May 10 to ~ 02:15 UT on May 11, the recovery phase was registered on May 11-13. Extremely intense geomagnetic disturbances, so-called "supersubstorms" (SSSs: SML < −2500 nT) were recorded during the superstorm. According to the SuperMAG data base, there were several SSS events: at ~19:20 and ~19:50 UT, ~22:35 and ~ 22:40 UT on 10 May, at ~09:00 and ~09:50 UT, at ~12:45, ~13:32 and ~13:43 UT on 11 May, 2024. The planetary space-time distribution of the magnetic disturbances during these SSS were studied using the data collected from the ground-based networks (SuperMAG, INTERMAGNET and IMAGE) as well as the magnetic registrations by the Iridium constellation of 66 satellites at 780 km altitude, distributed over six orbit planes spaced equally in longitude (AMPERE project). We studied the extremal geomagnetic disturbances during SSS by examining the morphology of the auroral electrojets, the corresponding positive magnetic bays at midlatitudes, and the solar wind driving conditions. Different features at mid-latitudes effects of these four SSS events are discussed.

Keywords: superstorm; supersubstorm; midlatitude positive bay

1. Introduction

Extreme geomagnetic storms provoked by geoeffective solar storms, has been recognized as a natural hazard [Weiler et al., 2025]. They may occasion widespread voltage control problems, power system collapse, transformer damage, pipeline damage, disruption of navigation by magnetic compass, satellite connection failures or change of satellite orbits. The geomagnetic storms are classified by two methods based on the k_p and Dst (SYM/H) geomagnetic indices. The NOAA geomagnetic storm scale includes five levels, by the storm effect on the different technologies. After this scale, the geomagnetic storms are classified from G1(k_p=5) to G5(k_p=9) [https://www.swpc.noaa.gov/noaa-scales-explanation]. The other type of classification is based on the Dst minimal value during the storm. The geomagnetic Dst index (Disturbance Storm Time) is a measure of the changes in the ring current flowing around the equator. The scale by Cander and Mihailovich (1998) offers 3 degrees of geomagnetic storm strength: moderate storm (-50 nT ≥ Dst ≥ -100 nT), intense storm (-100 nT ≥ Dst ≥ -250 nT), and super-storm (Dst ≤ -250 nT). Loewe and Prölss (1997) suggests a more detailed classification: weak storm (-30 nT ≥ Dst ≥ -50 nT), moderate storm (-50 nT ≥ Dst ≥ -100 nT), strong storm (-100 nT ≥ Dst ≥ -200 nT), severe storm (-200 nT ≥ Dst ≥ -250 nT), and great storm (Dst ≤ -350 nT). A geomagnetic storm may be classified as superstorm, if the Dst or SYM/H index reach values, lower from -450 nT or even -500 nT. Superstorms occur seldom. The recent superstorm on 10-12 May 2024 is the second by severity geomagnetic storm during the space era after the superstorm in 1989, and the only one for which simultaneous satellite data exist, together with the ground based data. This gives a unique opportunity to study different aspects of the reasons and conditions for the development of such phenomenon, to gain new knowledge, to verify and improve existing models, to plan new experiments in order to better predict such natural hazards. So, lots of papers concerning the superstorm on 10-12 May 2024 have been published [e.g. Haira et al., 2024; Wang et al., 2024; Lockwood et al., 2025; Weiler et al., 2025; Despirak et al., 2025; Kleimenova et al., 2025].

Another important element of the space weather is the magnetospheric substorms and their effects on the ionosphere and the ground magnetic field. Numerous studies have been devoted to this topic, starting with the classic work of Akasofu (1964). Magnetospheric substorms are associated with a series of processes in the magnetosphere and ionosphere, generalized by Akasofu (2004). Most of the substorm studies are related to the influence of substorms on the surface magnetic field, expressed in auroral latitude negative bays in X and positive bays, the so-called midlatitude positive bays (MPB) in the X magnetic component at midlatitudes [e.g., McPherron, 1972; McPherron and Chu, 2017)]. It was found that the strongest midlatitude positive bays occur during strong substorms, while strong geomagnetic storms develop [Guineva et al., 2024a; Guineva et al., 2024b].

The strength of the substorms is estimated by the global SML index, obtained by the SuperMAG magnetometers network. In the study of very strong magnetic substorms, a special class of substorms was identified, for which the name "supersubstorms" was introduced, and in which a number of phenomena are observed, distinguishing them from "ordinary" substorms. The so-called "supersubstorms" (SSS) are events during which the SML index reaches unusually low negative values (SML < -2500 nT) [Tsurutani et al., 2015]. Several of the most striking supersubstorm events have been examined in detail in detail by some authors of the present work [e.g. Despirak et al., 2022; Despirak et al., 2023; Lubchich et al., 2023].

During the superstorm on 10-12 May 2024 occured four supersubstorm events. These unique and rarely encountered extreme conditions allow for research and information to be gathered on the entire range of phenomena from the Sun to the Earth and on Earth that characterize extreme space weather.

The aim of this study is to conduct a detailed analysis of the geomagnetic auroral and midlatitude disturbances over Europe during the above-mentioned extremely disturbed conditions: the supersubstorms during the superstorm on 10–12 May 2024.

2. Data used

The interplanetary and geomagnetic conditions during the superstorm have been determined by data of OMNI database of the CDA Web (https://cdaweb.gsfc.nasa.gov/).

To obtain information about the ionospheric currents and consequently, about the western and eastern electrojet locations, we used data from AMPERE project (https://ampere.jhuapl.edu/products/) [Anderson et al. 2021; Waters et al. 2001]. It includes magnetic registrations by the Iridium constellation of 66 satellites at 780 km altitude, distributed over six orbit planes spaced equally in longitude and results from subsequent processing. Type 1 summary plots was used, which cover latitudes from 40° magnetic latitude (MLAT) to the pole to ensure coverage not only of the auroral reagon, but a considerable part of the midlatitudes, as well. All quantities are shown in Altitude Adjusted Corrected Geomagnetic Coordinates (AACGM). These summary plots display 10 minutes the input data, reduced magnetic perturbations showing the horizontal plane vectors (to the left), the horizontal vector from the spherical harmonic fit to the magnetic perturbation data (in the center), and the radial current density in μA/m2 (to the right). Upward currents are shown in red and downward currents in blue.

The supersubstorms have been identified by the SML index from SuperMAG (https://supermag.jhuapl.edu/) according to Tsurutani's definition [Tsurutani et al., 2015].

The magnetic field disturbances over Europe have been estimated by the regional IMAGE IL index for the PPN-NAL chain, wich is near the longitude of Panagjurishte. The PPN-NAL area covers longitudes from 12°÷27°E (96°-113° GMLon.). The IL index is available in the IMAGE database (https://space.fmi.fi/image/www/il_index_panel.php).

The midlatitude disturbances during the studied period have been taken from the Catalog of the magnetic variations at the Panagjurishte station (PAG), developed at the Space Research and Technology Institute of the Bulgarian Academy of Sciences, based on INTERMAGNET data (https://imag-data.bgs.ac.uk/GIN_V1/GINForms2). The catalog is available at: http://space.bas.bg/Catalog_MPB/. The Panagjurishte (PAG) coordinates are: 24.2°E, 42.5°N (96.8°GMLon., 37° GMLat.). For the study the processed X component at PAG representing the X variations (delta X) obtained based on 25 days period with the considered day in the center is used. The developed processing procedure includes removal of the main field, removal of gaps and peaks, subtraction of the solar quiet day variationsand elimination of days with strong disturbances [Werner et. al. 2021]. Graphs of the midlatitude positive bays, detected based on the created methodology, are used, as well [Guineva et al., 2024c].

To compare the substorm by the midlatitude positive bays (MPB's), registered at PAG, with general substorm development at the same time, the substorm list by Forsyth et al. (2015), has been used (https://supermag.jhuapl.edu/substorms/?tab=description), SML index from SuperMAG (https://supermag.jhuapl.edu/indices/) and IL index data from IMAGE database (https://space.fmi.fi/image/www/il_index_panel.php).

3. Interplanetary and geomagnetic conditions

3.1. The superstorm on 10-12 may 2024

The superstorm on 10-12 May 2024 appears a huge magnetic storm (superstorm) of class G5 (Kp = 9) and a minimal value of the hourly index Dst equal to -412 nT, at 02:00 UT on 11 May, 2024 (http://wdc.kugi.kyoto-u.ac.jp/), and the minimal value of the minute analogue of Dst, the Sym/H reached -518 nT at 02:14 UT on 11 May 2014. The most intensive superstorm in the space era was the superstorm on 13-14 March 1989, with minimal Dst=-589 nTat 00:02 UT on 14 March 1989, and minimal SYM/H= -720 nT at 00:46 UT on 14 March 1989. Such a strong magnetic storm as the superstorm on 10-12 May 2024 has not been observed for more than 20 years. In terms of intensity, it is comparable to the strongest magnetic storms observed since the beginning of the space era, namely the storms of September 1957 (Dstmin = −427 nT), February 1958 (Dstmin = −426 nT), July 1959 (Dstmin = −429 nT) and November 2003 (Dstmin = −422 nT, SYM/Hmin=490 nT) (Kleimenova et al., 2025). The superstorm on 10-12 May 2024 is the first one about which simultaneous satellite data alog with ground data have been registered. It was provoked by a solar storm in May 2024. A series of eruption events occurred in May 2024, which are associated with AR13664/8. This active region revealed the appearance of an extremely intense magnetic flux, lasted for 3 days, and gave rise to multiple flares of class M and 4 flares of class X. Each flare was accompanied by halo CME.

The source regions of seven halo CMEs were determined, apportioned mainly along two distinct polarity inversion lines, leading to two groups of homologous CMEs. The strong flux emergence was the reason to a complex magnetic field configuration in the region [Wang et al., 2024]. By combined satellite data five CMEs in the frame of 28 hours, interacting with each other were identified near Earth, thus creating an interplanetary magnetic field with a very complex structure [Weiler et al., 2025]. This intricate near-Earth solar wind and IMF structure aroused the superstorm in May 2024 with a complex structure, as well. The superstorm had a three-step storm main phase, from ~17:15 UT on May 10, lasted ~9 hours, with SYM/H intensity of -518 nT. Due to 3 MC during the superstorm recovery phase it was very structured and prolonged to 2.8 days. Strong field-aligned polar region currents, ~10 times intensified during the main phase, with equatorward expansion to ~50° Mlat. [Haira et al., 2024]. During the superstorm, lots of intense substorms and several supersubstorms occurred. In Figure 1, the interplanetary and geomagnetic conditions from 10 to 14 May 2024 are shown. From up to down, the IMF B, the N-S IMF component Bz, the solar wind parameters: velocity V, proton density Np, temperature T, pressure P, and the AL and SYM/H indices are presented.

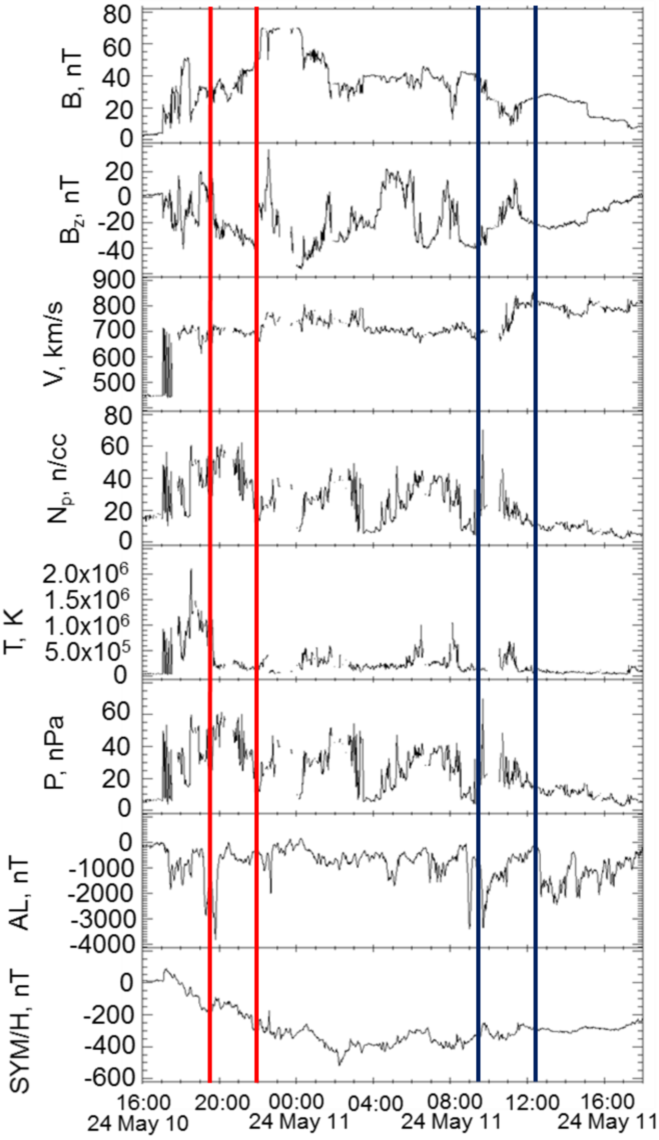

Figure 1. *Interplanetary and geomagnetic conditions during the superstorm on 10-12 May 2024. The red vertical lines indicate the beginnings of the midlatitude positive bays, observed at the midlatitude station Panagjurishte, associated with the first and second SSS event during the main phase of the superstorm, on 10 May 2024 (see sections 4.2, 5.3 and 6.3). The blue vertical lines mark the beginnigs of the negative bays, recoded at PAG, during the superstorm recovery phase, related to the third and fourth SSS events on 11 May 2024 (see sections 4.2, 7.3 and 8.3).*

3.2. The supersubstorms during the superstorm on 10-12 May 2024

We determined the onset and maximal development of the SSSs during the 10-12 May 2024 superstorm by the SML index from SuperMAG database and compared our results with the SuperMAG substorms lists (when available). In Figure 2 the SML course from 16 UT on 10 May 2024 to 24 UT on 11 May 2024 is given. Four SSS events were identified in this time interval, enumerated in Figure 2 and further in the text from (1) to (4). Two SSS events occurred on 10 May 2024, during the main storm phase, and two SSS events developed on 11 May 2024, in the recovery storm phase. Three of the SSS events, (1), (3) and (4), consist of two consecutive SSSs, which may partly overlap, so the precise onset time of the second SSS may be hard to determine. SSS event (2) represents one SSS.

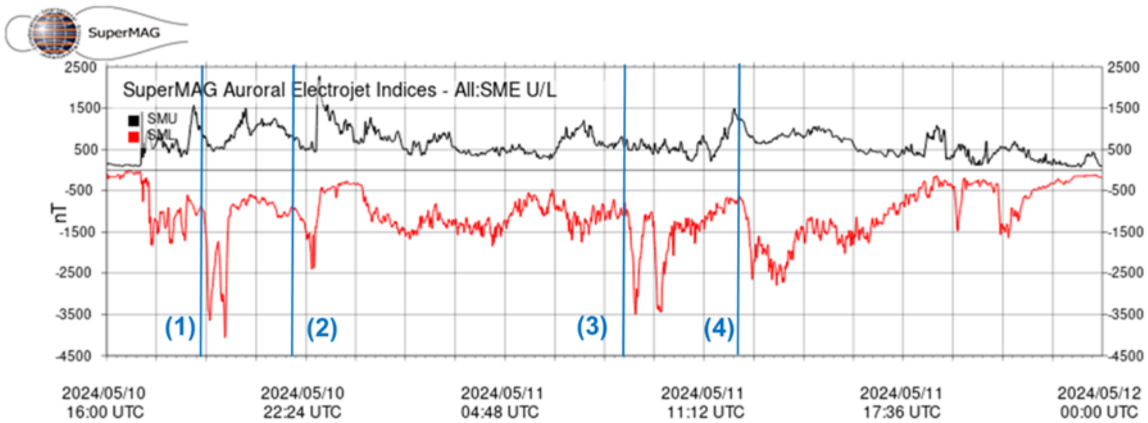

Figure 2. *SML and SMU indices by SuperMAG. The beginnings of the SSS events are marked by blue vertical lines and the SSS are enumerated by the time of occurrence.*

The onset times and the times of the maximal development and the intensity of the SSS events were determined as follows:

SSS event (1): The onset of the first SSS was at 19:03 UT on 10 May 2024, it reached maximal development at 19:19 UT with intensity -3649 nT. The onset of the second SSS was at 19:35 UT, and the maximal development - at 19:48 UT with intensity -4057 nT.

SSS event (2): The onset of the SSS (one for this event) was at 22:04 UT on 10 May 2024. At the maximal development, there are two close to each other minima: at 22:36 UT, with intensity -2404 nT, and at 22:40 UT, with intensity -2369 nT.

SSS event (3): The onset of the first SSS was at 08:39 UT on 11 May 2024, its maximal development was at 09:00 UT with intensity -3497 nT. The onset of the second SSS was at 09:25 UT, and the maximal development - at 09:50 UT with intensity -3433 nT.

SSS event (4): The onset of the first SSS was at 12:20 UT on 11 May 2024, it reached maximal development at 12:45 UT with intensity -2650 nT. The onset of the second SSS was at 13:04 UT. The SML curve is more disturbed, at the maximal development two close minima were obtained: at 13:32 UT with intensity -2797 nT, and at 13:43 UT with intensity -2722 nT.

4. First SSS event

4.1.AMPERE data

During the superstorm, the current systems are very strong and very complicated. [Haira et al., 2024] report, that there was obtained ~10 times increase of the upward- and downward-current components in both the northern and southern hemispheres during the storm period, compared to their pre-storm values. The high intensity and complex structure of the current systems are clearly visible in all figures for the moments of maximal development of the supersubstorms considered in our work.

In Figure 3, AMPERE data around the maximal SSS developments for the first SSS event are given. The maximal developments times are written in black frames below the data time interval. Here and in the following slides, the stars indicate the SSS onset location (taken from the Forsyth et al. substorms list [Forsyth et al. 2015]), and the ellipses – the region of the PPN-NAL and PAG stations. In this case, the SSS onsets are at a distance of about 200° from the PPN-NAL region (onset 1: 8.21 MLT, 60°GMLat; onset 2: 8.86 MLT, 67° GMLat). During the first SSS the current systems are concentrated above 55°-50° GMLat. It is seen, that the westward electrojet doesn't reach the European stations area (upper row of Figure 3). During the second SSS part of the westward electrojet is above the PPN-NAL region, namely over Spitsbergen archipelago.

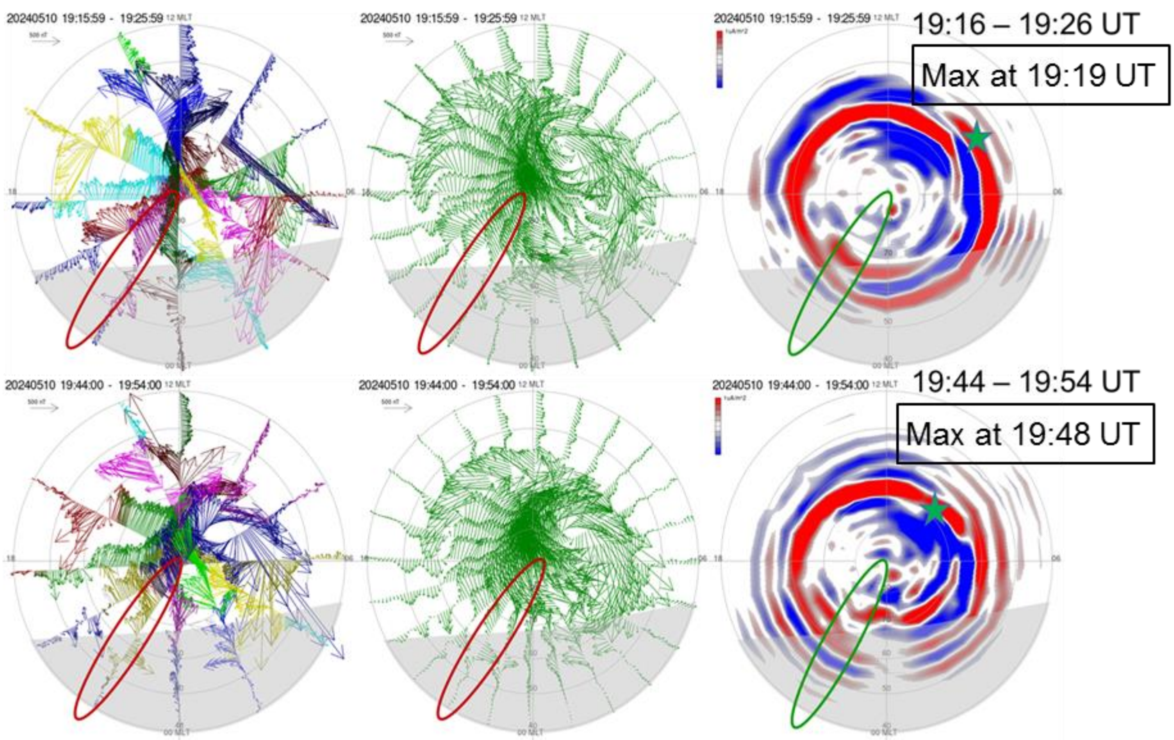

Figure 3. *AMPERE data around the SML minima times of the two SSSs of the first SSS event. The green stars indicate the SSS onsets (GMLat, MLT) and the ellipses – the location of the European magnetic stations at the same time.*

4.2.SuperMAG and IMAGE data

To study the magnitude and the overall distribution of the ground level magnetic field horizontal perturbations we used the polar plots from SuperMAG from 30° GMLat to the GM pole. The vectors are rotated 90° clockwise to show the ionospheric equivalent current direction. The uniformly gridded fitted vectors in an MLT-MLat grid rotated also 90° clockwise are drawn as well. The ground magnetic variations over Europe have been studied by data of the IMAGE stations.

In the left panel of Figure 4 the SuperMAG maps for the time of the first and second supersubstorm onsets and maximal developments are presented. It can be seen that the strongest magnetic disturbances are far from the PPN-NAL area. During the first SSS, only weak and chaotic disturbances are observed at European longitudes, and during the second SSS stronger disturbances can be seen only at very high latitudes.

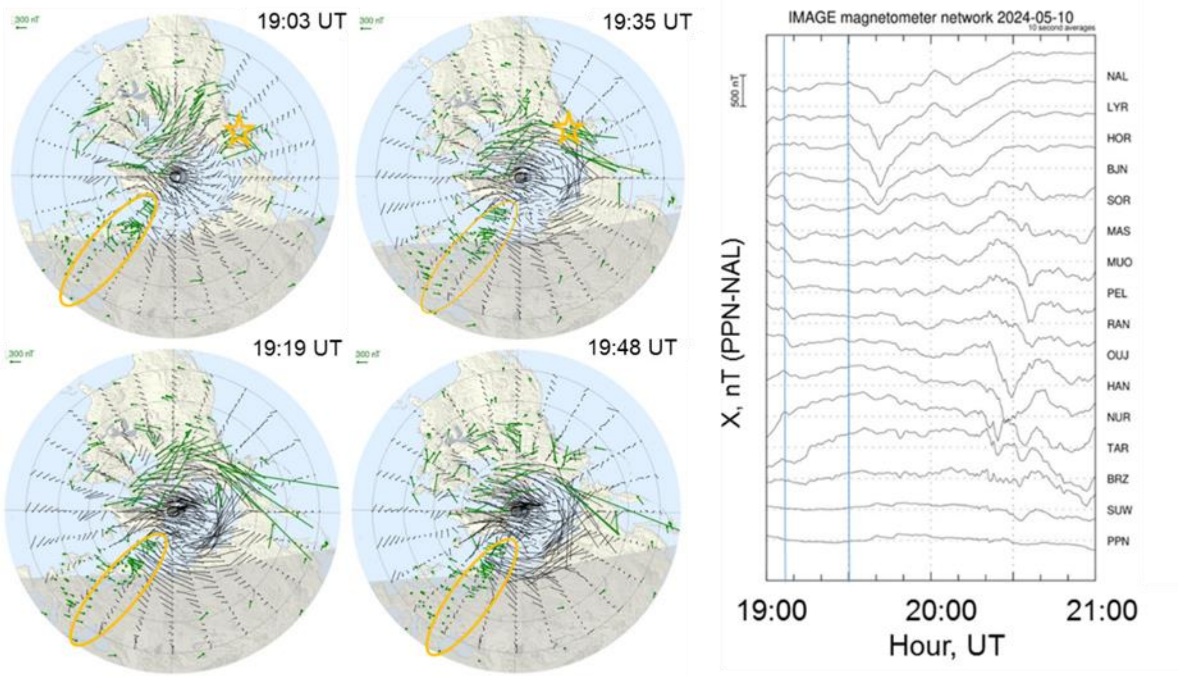

Figure 4. *Maps of the magnetic field vectors by SuperMAG for the onset and maximal development of the first SSS (left column) and of the second SSS during the first event (right column). The orange stars mark the supersubstorms onsets and the ellipses – the location of the IMAGE PPN-NAL stations and PAG. In the right panel, X magnetic component from the PPN-NAL chain stations is given from 19:00 to 21:00 UT on 10 May 2024. The blue vertical lines indicate the substorm onsets.*

From the right panel of Figure 4 it can be seen, that during the first disturbance, only weak X variations are observed in the auroral region, and during the second SSS a so-called "polar" substorm develops [Kleimenova et al., 2023; Despirak et al., 2025]. These results are in complete agreement with the ionospheric currents distribution by AMPERE (Figure 1), where part of the westward electrojet was just over the Spitsbergen archipelago.

4.3. First SSS event by SML, IL and magnetic X variations at PAG

In Figure 5 the global SML index and the auroral and midlatitudes disturbances of the regional IL PPN-NAL index and the variations of the X component of the magnetic field at PAG during the first SSS event are presented.

In the upper graph of Figure 5 the SML index is shown from 19 to 21 UT on 10.05.2024. The two SSS are clearly expressed. The SSS onsets are at a great distance from the PPN-NAL region, about 200° in longitude, in East direction. During the first SSS, with onset at 19:03 UT, the westward electrodjet didn't reach European longitudes at the maximal SSS development, so there was no visible effect at auroral latitudes, as it is expressed by the IL graph for the same time interval (below SML graph in Figure 5). The X variations at PAG (the bottom panel of Figure 5) also do not reflect any influence of the first SSS at midlatitudes.

During the second SSS disturbances at high European latitudes were observed, by the IL index the disturbance began at 19:30 UT, somewhat earlier from the SML determined onset (19:35 UT), but such small discrepancy is not surprising, as the second SSS arose immediately after the first one, in already very disturbed conditions, which troubles the accurate determination of the SSS onset. At the maximal development at 19:42 UT IL= -1050 nT. This disturbance is comparatively small versus the global disturbance (-4057 nT), as the strongest disturbances happened to the East, in Asia. At PAG, the beginning of the disturbance provoked by the SSS was from 19:24 UT, and a strong midlatitude positive bay (MPB) formed, with maximal value of 74.6 nT.

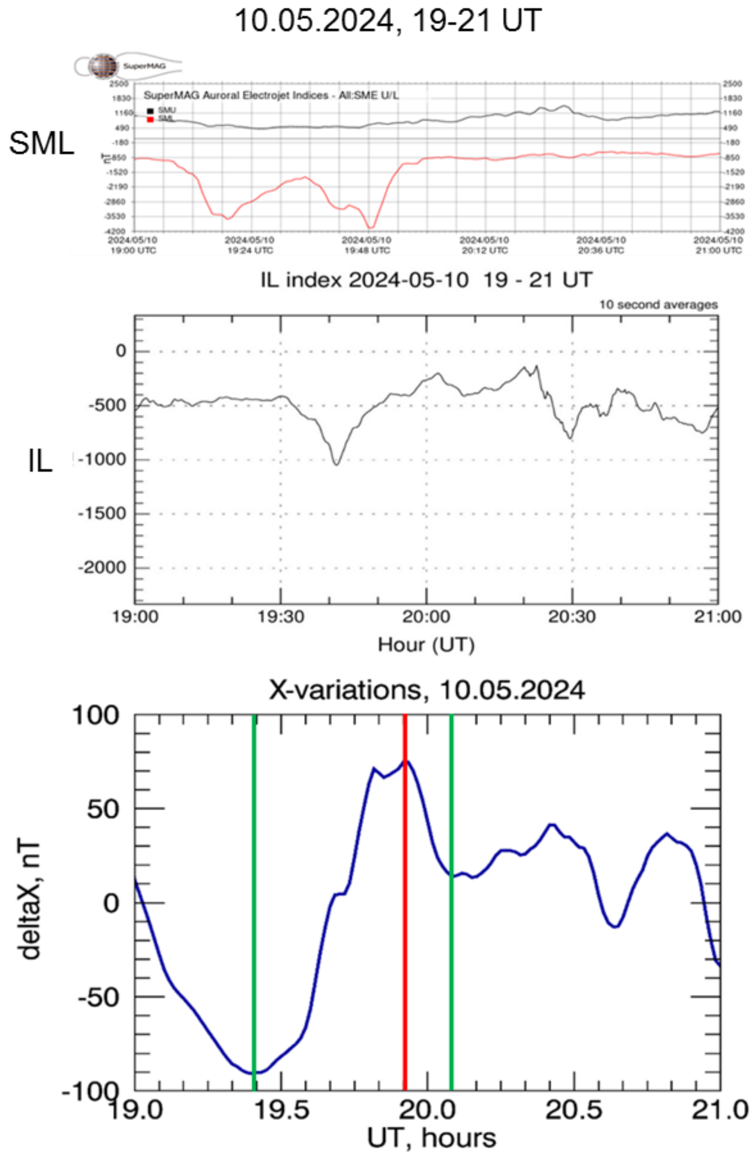

Figure 5. *SML index (up), IL index (down), and X variations at PAG (further down) from 19 UT to 21 UT on 10.05.2024. The green vertical lines in the bottom panel indicate the beginning and end of the MPB registered at PAG, and the red vertical line – the time of the MPB maximum.*

5. Second SSS event

5.1.Second SSS event by AMPERE data

The second SSS event consists from one supersubstorm, its onset was at 22:04 UT on 10 May 2024, and the onset location was at 8.21 MLT, 54° GMLat (Forsyth et al. substorms list [Forsyth et al. 2015]). In Figure 6 the distribution of the ionospheric currents near the time of maximal development, at 22:36 UT and 22:40 UT. It is seen that the area of the current systems expanded to lower latitudes and reached and maybe surpassed 40° GMLat. The PPN-NAL area falls under the westward electrojet.

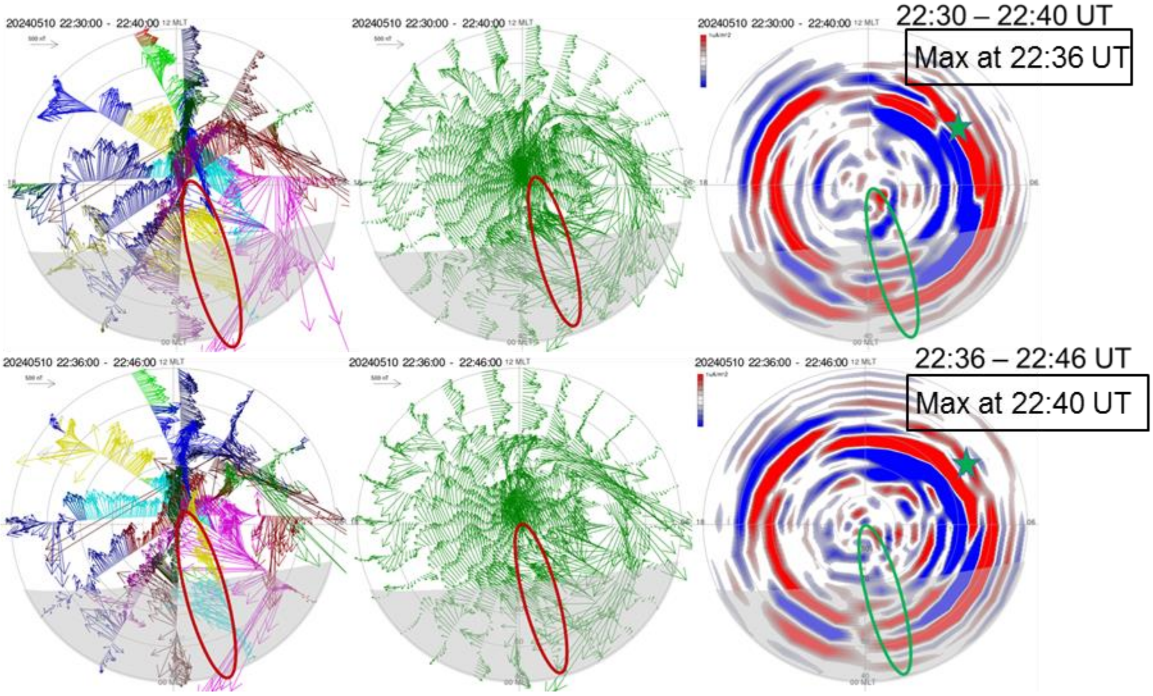

Figure 6. *Field aligned ionospheric currents at the time of the maximal development of the supersubstorm of the second SSS event. All designations are as in Figure 3.*

5.2.Second SSS event by SuperMAG and IMAGE data

In Figure 7 maps of the magnetic perturbations at the onset and near the maximal

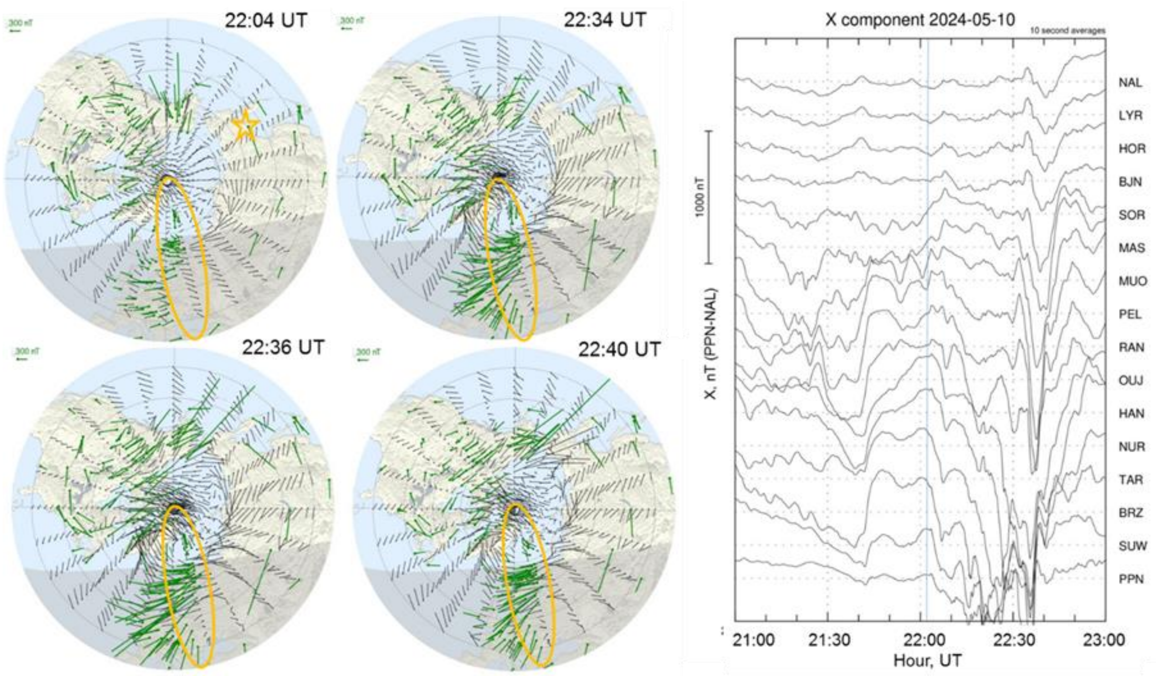

Figure 7. *Maps of the magnetic perturbations at the onset and near the maximal development of the second SSS event (left panels) and X components variations at the IMAGE PPN-NAL chain stations (right panel). All designations are as in Figure 4.*

development during the supersubstorm at 22:04 UT on 10.05.2024 (left panel) and the X magnetic component at the PPN-NAL chain stations from 21 UT to 23 UT (right panel) are shown.

From the maps it is seen, that magnetic disturbances are seen to span all longitudes and the strongest ones are over Europe, at subauroral and middle latitudes. During the second SSS event, IMAGE region is at about 1 MLT. In the X magnetograms the onset and further development of the SSS is evident.

5.3. Second SSS event by SML, IL and magnetic X variations at PAG

In Figure 8 the second SSS event is shown by the SML index (upper graph), by the IL PPN-NAL index (middle graph) and by the X variations at PAG (bottom graph).

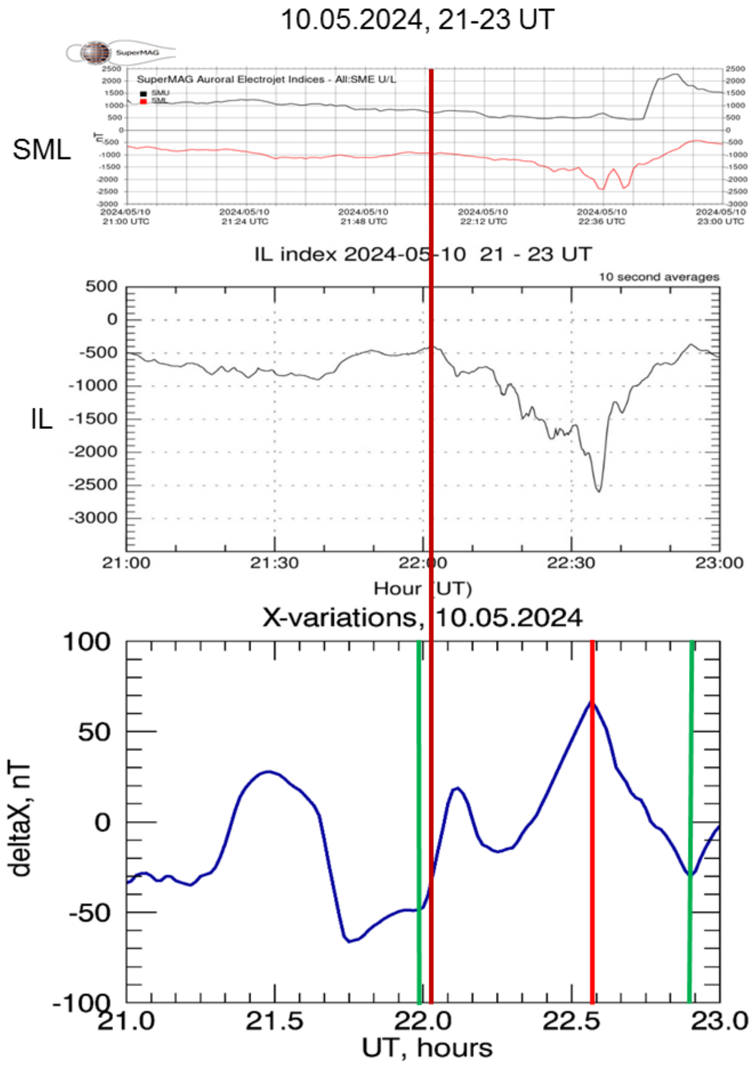

Figure 8. *SML index (up), IL index (down), and X variations at PAG (further down) from 21 UT to 23 UT on 10.05.2024. The dark red vertical line indicates the SSS onset, the green vertical lines in the bottom figure mark the beginning and end of the MPB at PAG, and the red vertical line – the maximum of the MPB.*

Although the defined onset of the SSS is at a distance of over 100° by longitude to the East from the IMAGE region (see Figure 6, 7), the beginning of the magnetic disturbance at European auroral latitudes at 22:04 UT coincides with the SSS onset (middle graph of Figure 8), and it is close in magnitude to the global disturbance determined by the SML. The SSS intensity by SML is -2404 nT, and by IL it is -2600 nT, both at 22:36 UT. The slightly higher regional SSS intensity value confirms that the strongest disturbances occurred over Europe.

A strong MPB at PAG is obtained, with beginning close to the SSS onset (at 21:58 UT, 6 min. earlier than the determined onset, see left green line in the bottom graph of Figure 8). The MPB maximal value was 66.8 nT.

6. Third SSS event

6.1.Third SSS event by AMPERE data

The third SSS event was observed during the recoveri phase of the superstorm, on 11.05.2024. It consists of two consecutive SSS with onsets at 8:39 UT (2.27 MLT, 54° GMLat) and 9:25 UT (1.98 MLT, 67° GMLat; Forsyth et al. sustorms list [Forsyth et al. 2015]). The SSS onsets are in the night sector, and the PPN-NAL area in this case is in the day sector. Usually at that time the PPN-NAL area should lie under the Eastward electrojet. In Figure 9 the AMPERE data near the maximal development of the two supersubstorms are given. All designations are as in Figure 3. By the current systems distribution it is seen, that at the first SSS maximal development the current configuration is rather complex, presenting several alternating slices of downward and upward currents with different intensity and boundaries (upper right image in Figure 9, the green ellipse). At the second SSS maximal development the PPN-NAL area lies under Eastward electrojet current structure (bottom right image in Figure 9, the green ellipse).

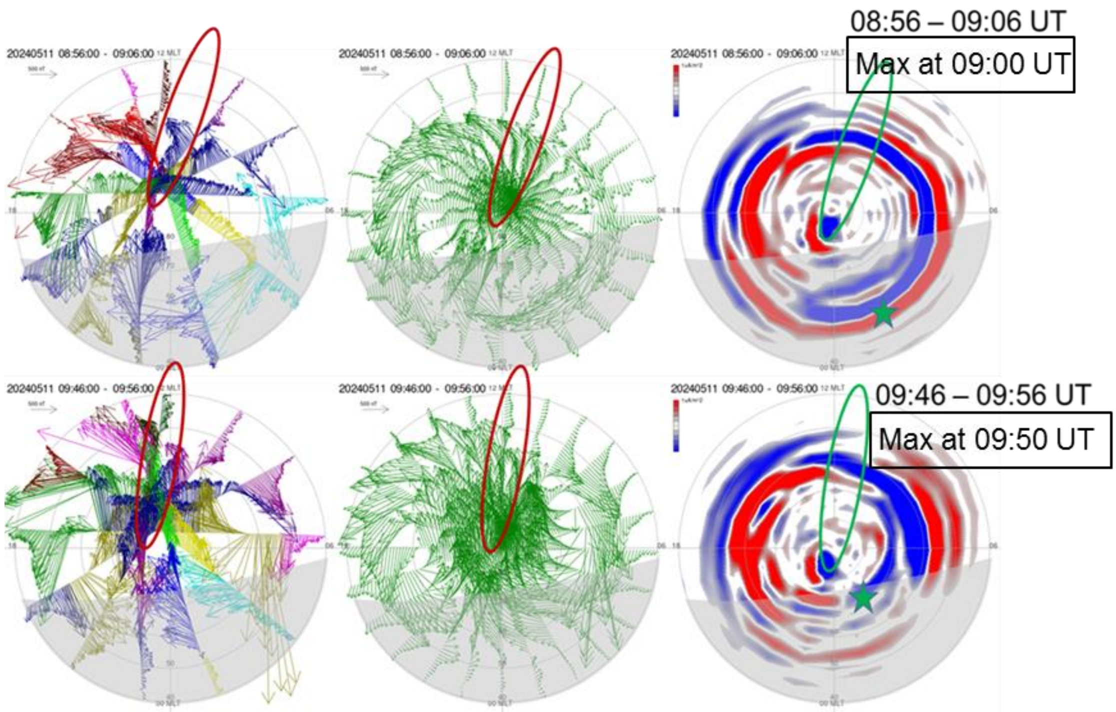

Figure 9. *AMPERE data at the time of the maximal development of the supersubstorms of the third SSS event during the superstorm. All designations are as in Figure 3.*

6.2.Third SSS event by SuperMAG and IMAGE data

The ground magnetic field variations during the third SSS event are presented in Figure 10. From the maps it is seen, that the main disturbances were in the night sector. The IMAGE stations get into the day sector. There are magnetic disturbances, but they seem rather chaotic. By the PPN-NAL graphs in the course of X, weak maxima can be observed in the auroral region after the onset of supersubstorms (blue vertical lines in the right panel), which spread to higher and lower latitudes, but do not stand out against the background of disturbances during the examined period.

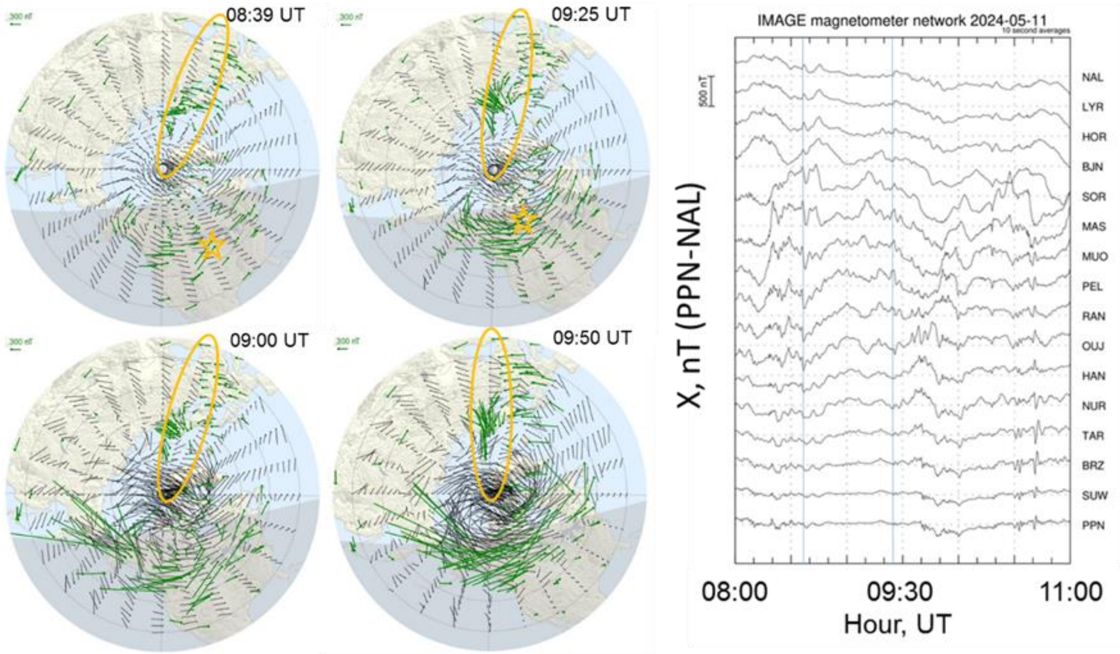

Figure 10. *Maps of the magnetic field vectors (left panel) at the onset (upper row) and maximal development (bottom row) times of the first SSS (left column) and second SSS (right column) of the third SSS event and X component variations at the IMAGE PPN-NAL stations from 08 UT to 11 UT on 11.05.2024 (right panel).*

6.3. Third SSS event by SML, AL, IL and magnetic X variations at PAG

The third SSS event and its effect at European auroral and midlatitudes are shown in Figure 11. From up to down the following quantities are presented: the global SML index, the global AL index, the regional IU and IL indices, and the X variations at the midlatitude station PAG. The two supersubstorms during the event are clearly expressed by the global indices. The SML and AL indices have the same shape and intensity. The behavior of the SML index is described in section 4.2. AL index also shows two-minima structure, with min at 09:00 UT and 09:44 UT, and corresponding values ~ -3400 nT and ~ -3380 nT, which is near the SML result.

By the IU index, near the maximal development of the first SSS a very small positive bay is observed, several times smaller than the neighboring positive disturbances. During the second SSS, a weak positive bay is obtained in the IU index, related to the eastward electrojet above the stations.

In addition, at Panagjurishte (PAG) (24.2°E, 42.5°N) there are no significant deviations in the X variations, either positive or negative, during the first SSS. But a negative bay is observed at ~09:50 – 10 UT, reaching -75 nT, which may be associated with the spreading current of the eastward electrojetde.

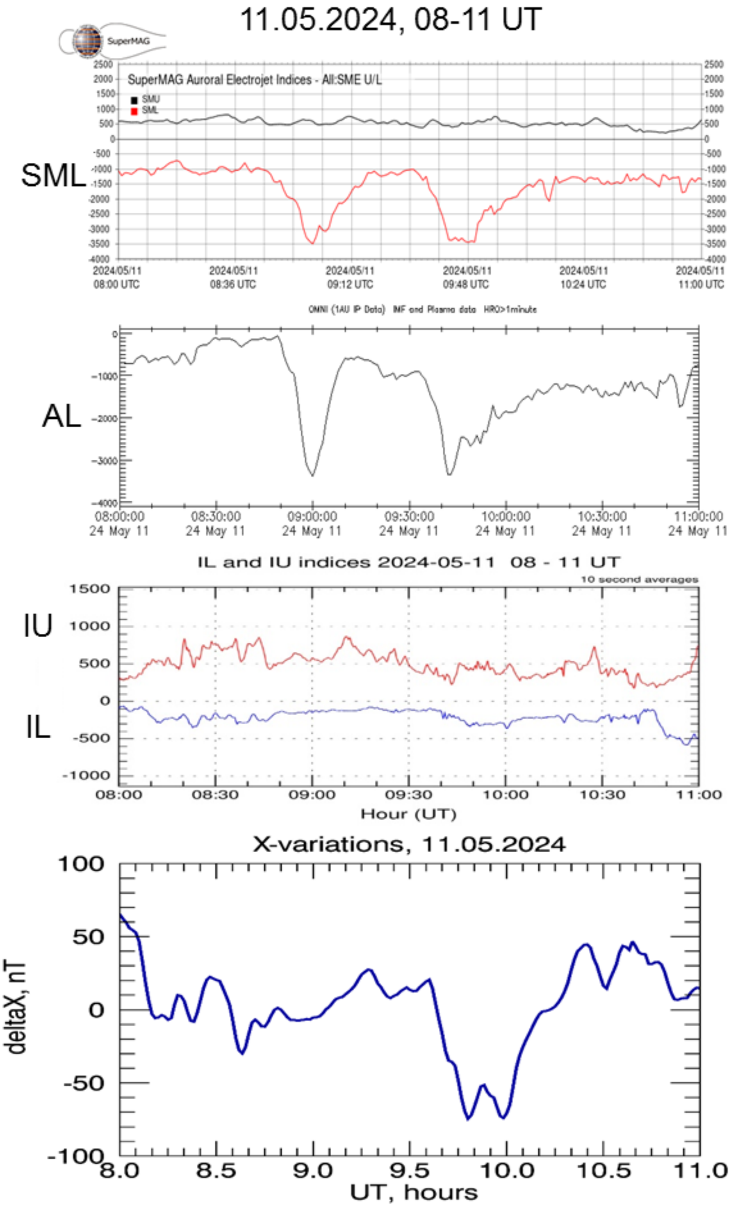

Figure 11. *From up to down: SML, AL, IU and IL indices, and X variations at PAG station from 8 UT to 11 UT on 11.05.2024.*

7. Fourth SSS event

7.1.Fourth SSS event by AMPERE data

The fourth SSS event occurred during the recovery phase of the superstorm, on 11.05.2024, and the European area lay in the evening MLT sector, under the eastward electrojet. The westward electrojet developed over America. In Figure 12 the AMPERE data near the maximal development of the two supersubstorms are presented. In the first row data about the first supersubstorm are given. The onset was at 3.48 MLT, 57° GMLat, and the maximal development at 12:45 UT. The second and third row show data near the maximal development of the second supersubstorm, for which two near SML minima were detected: at 13:32 UT (second row of Figure 12) and 13:43 UT (third row of Figure 12). The SSS onset was at 3.74 MLT, 67° GMLat. The field aligned currents were strong.

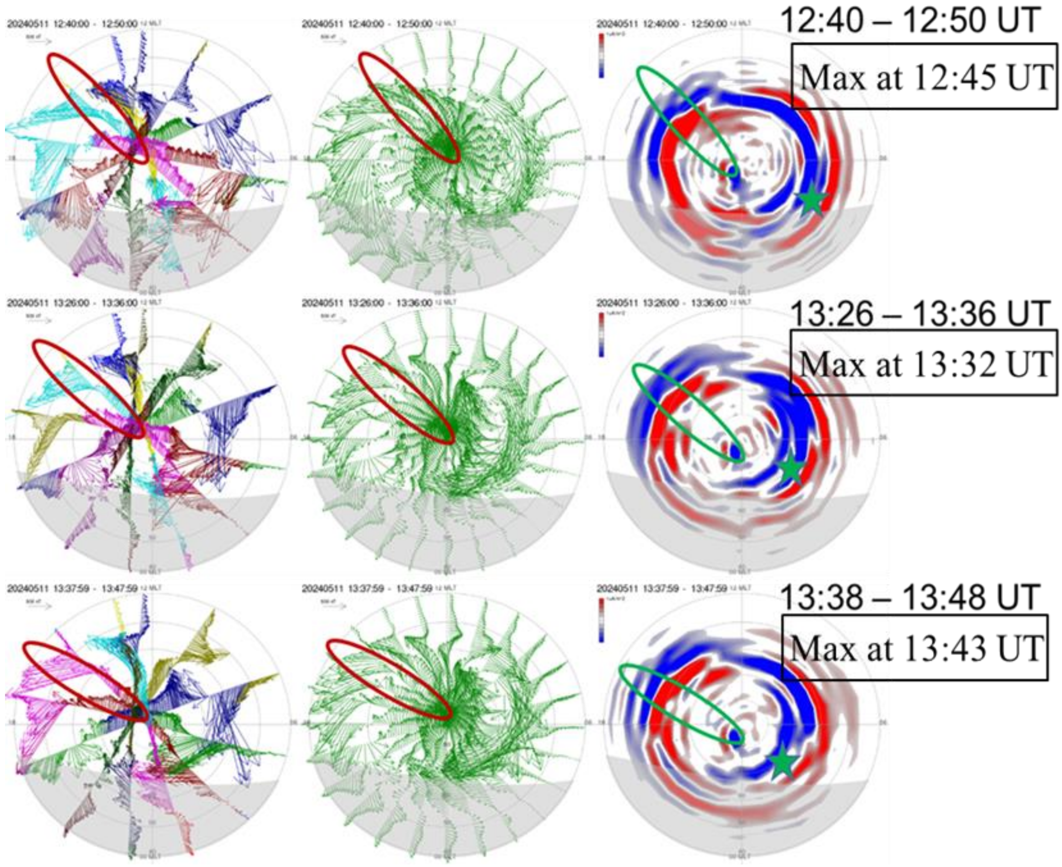

Figure 12. AMPERE data near the maximal developments of the first SSS (upper row) and second SSS (middle and bottom row) of the fourth SSS event on 11 May 2024. All designations are as in Figure 3.

7.2. Fourth SSS event by SuperMAG and IMAGE data

The ground magnetic variations during the fourth SSS event are shown in Figure 13. The left panel presents the maps of the magnetic vectors at the onsets (upper row) and maximal developments (bottom row) of the two supersubstorms. The right panel shows the X component of the magnetic field at the PPN-NAL chain stations from 11 UT to 16 UT on 11.05.2024.

During the first SSS IMAGE stations were under the eastward electrojet and positive bays in the X component at auroral latitudes were registered. During the second SSS, the magnetic vector orientation is more chaotic and some effect in X of the PPN-NAL chain did not appear.

7.3. Fourth SSS event by SML, AL, IL and magnetic X variations at PAG

The Fourth SSS event and its appearance at European auroral and midlatitudes are presented in Figure 14. In the panels from up to down the SML index, the AL index, the regional (for Europe) IU and IL indices, and the X variations at the midlatitude station PAG are presented. The two supersubstorms during the event are clearly seen by the course of the global indices.

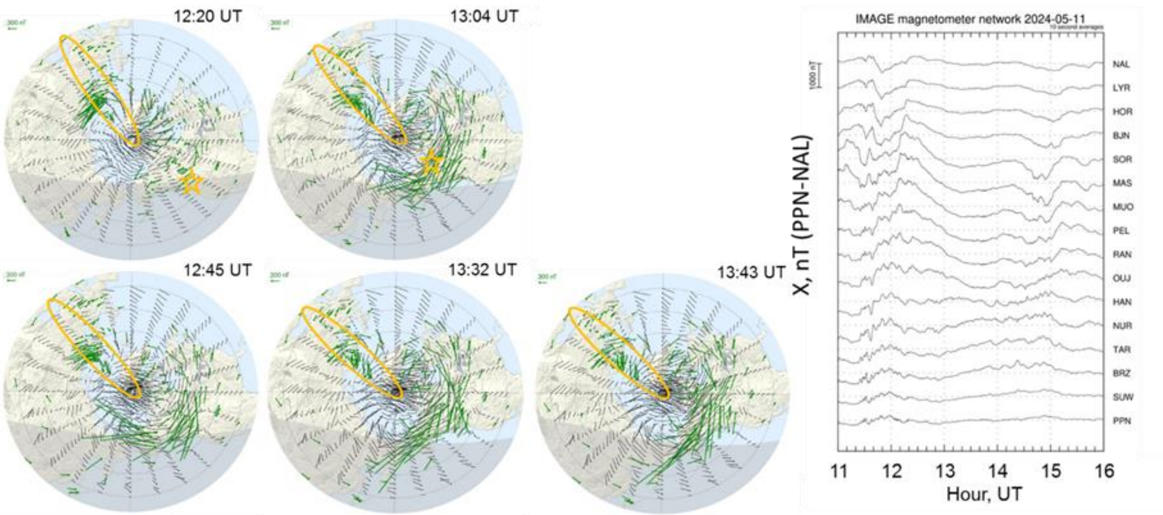

Figure 13. *SuperMAG maps of the magnetic perturbations (left panel) at the onset (upper row) and maximal development (bottom row) of the two SSSs from the fourth SSS event during the superstorm and X component of the magnetic field at the PPN-NAL stations from 11 to 16 UT (right panel).*

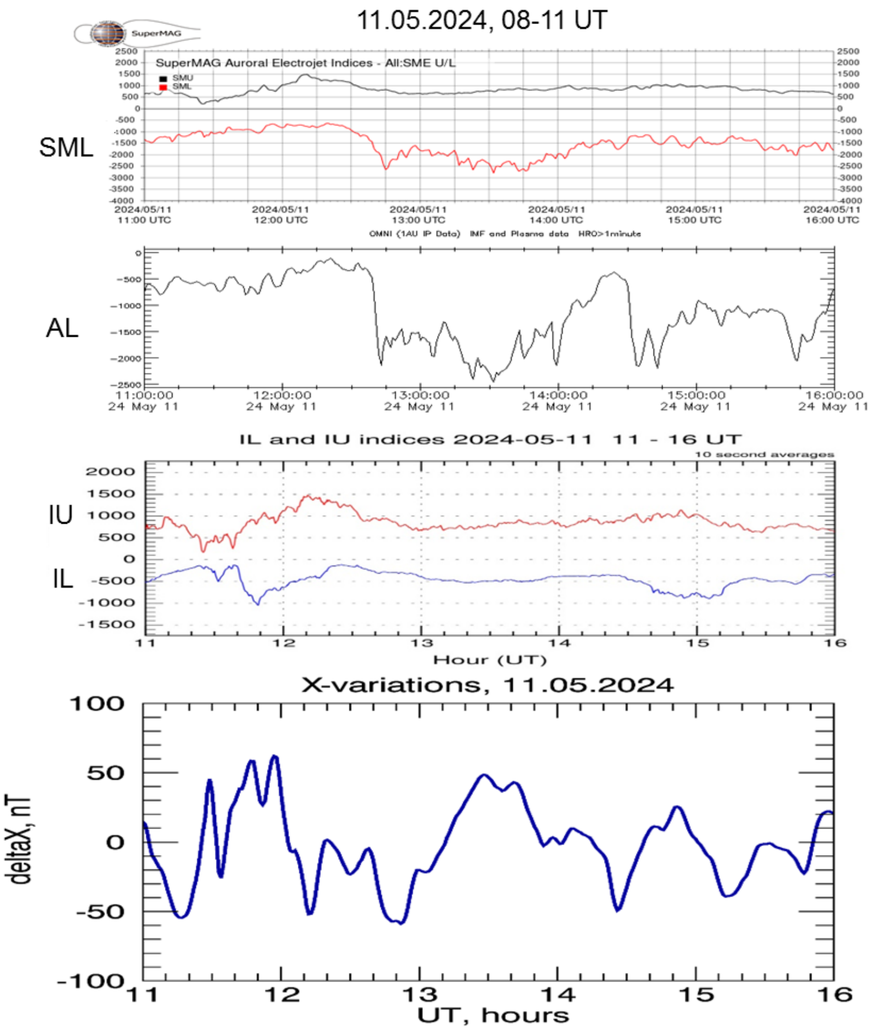

Figure 14. *SML (up), AL (down), IL and IU indices (further down), and X variations at PAG (bottom) from 11 UT to 16 UT on 11.05.2024.*

The SML and AL indices follow the same shape. The SSSs parameters by SML index are described above, in section 4.2. AL index shows a similar structure, with minima at 12:46 UT for the first SSS, 13:26 UT and 13:34 UT for the second SSS, and corresponding intensities ~ -2180 nT and ~ -2400 nT, and 2490 nT.

By IMAGE PPN-NAL IU index (96°-113° GMLon.) a positive peak is observed during the first SSS, related to the increasing of the eastward electrojet. Perhaps because the event is not isolated the increasing of the eastward electrojet was not recorded during the second SSS

At Panagjurishte (PAG) 24.2°E, 42.5°N) a minimum is observed during the first SSS, reaching -60 nT.

8. Summary

Auroral and midlaltitude disturbances observed by four supersubstorm events during the superstorm on 10-12 May 2024 have been examined. The planetary distribution of ionospheric currents, typical for SSS, confirmed the previous results: development of both westward and eastward electrojets on a global scale, encompassing the Earth from different sides was observed. During the main storm phase, the southern boundary of the field aligned currents reaches and maybe surpasses 40° GMLat. The field aligned currents manifest sometimes a very complicated structure, in most areas consisting of alternating slices of upward and downward currents.

The magnetic variations in the PPN-NAL and PAG longitudinal regions (12°-25°E; 96°-113° GMLon) have been considered.

When the PPN-NAL area is in the night MLT sector (the events on 10.05.2024) and the westward electrojet reaches it, negative bays in X are registered at auroral latitudes.

When the PPN-NAL area is in the day MLT sector, if the eastward electrojet is above the IMAGE stations, positive bays in X are observed.

Note that our study of midlaltitude positive bays (MPB) was confined to the analysis of data from only one station - PAG. It should be also noted that The MPB's during extremely disturbed conditions are typically of complicated form, in many cases they are composed of two or more maxima, sometimes with deep minima between them, which may bother the processing. Typically, data under highly disturbed conditions is highly noisy, both due to unusual rapid strong variations in the data and perhaps also due to ambient conditions. This sometimes requires additional specific processing and verification.

When the SSS is observed in the PPN-NAL area, in the night MLT sector, its effect is clearly expressed at midlatitudes (PAG), with a MPB beginning near the drop of IL index and high X_{max} values (above 50 nT).

When PAG was in the day MLT sector, no effect was observed when there is not a clearly expressed maximum in the IU index, and a significant decrease in X (of the range of -60÷ -70 nT) was obtained if the PPN-NAL region is below the eastward electrojet.

Acknowledgements: We acknowledge the substorm timing list identified by the Newell and Gjerloev technique, the SMU and SML indices (Newell and Gjerloev, 2011); and the SuperMAG collaboration (Gjerloev et al. 2012). The authors are grateful to the creators of the databases AMPERE (https://ampere.jhuapl.edu/), IMAGE (http://space.fmi.fi/image/), OMNI (https://cdaweb.gsfc.nasa.gov/), and INTERMAGNET (http://intermagnet.org/) for the opportunity to use them in this work.

References

Akasofu, S.-I. (1964). The development of the auroral substorm, *Planetary and Space Science*, Vol. 12, No. 4, pp. 273–282.

Akasofu, S.-I. (2004). Several 'controversial' issues on substorms, *Space Science Reviews*, Vol. 113, pp. 1–40, DOI: 10.1023/B:SPAC.0000042938.57710.fb.

Anderson, B.J., Angappan, R., Barik, A., Vines, S.K., Stanley, S., Bernasconi, P.N., Korth, H., Barnes, R.J. (2021). Iridium Communications Satellite Constellation data for study of Earth's magnetic field, *Geochemistry, Geophysics, Geosystems*, Vol. 22, e2020GC009515, DOI: 10.1029/2020GC009515.

Cander, L.R., Mihajlovic, S.J. (1998). Forecasting ionospheric structure during the great geomagnetic storms, *Journal of Geophysical Research: Space Physics*, Vol. 103, No. A1, pp. 391–398, DOI: 10.1029/97JA02418.

Despirak, I.V., Lubchich, A.A., Kleimenova, N.G., Setsko, P.V., Werner, R. (2022). Supersubstorm on 20 December 2015: Spatial geomagnetic effects, *Proceedings of the Fourteenth Workshop "Solar Influences on the Magnetosphere, Ionosphere and Atmosphere"*, pp. 10–15, DOI: 10.31401/WS.2022.proc.

Despirak, I.V., Lubchich, A.A., Kleimenova, N.G. (2023). Space weather conditions and non-storm supersubstorms observations, *Proceedings of the Fifteenth Workshop "Solar Influences on the Magnetosphere, Ionosphere and Atmosphere"*, pp. 35–40, DOI: 10.31401/WS.2023.proc.

Despirak, I.V., Kleimenova, N.G., Lubchich, A.A., Setsko, P.V., Malysheva, L.M. (2025). "Polar" substorms during slow solar wind, *Journal of Geophysical Research: Space Physics*, Vol. 130, e2024JA033555, DOI: 10.1029/2024JA033555.

Despirak, I.V., Setsko, P.V., Lubchich, A.A., Sakharov, Y., Selivanov, V. (2025). Geomagnetically induced currents (GICs) during the strong geomagnetic storm on 10–12 May 2024, *Advances in Space Research*, in press, DOI: 10.1016/j.asr.2025.06.081.

Forsyth, C., Rae, I.J., Coxon, J.C., Freeman, M.P., Jackman, C.M., Gjerloev, J., Fazakerley, A.N. (2015). A new technique for determining substorm onsets and phases from indices of the electrojet (SOPHIE), *Journal of Geophysical Research: Space Physics*, Vol. 120, No. 12, pp. 10592–10606, DOI: 10.1002/2015JA021343.

Gjerloev, J.W. (2012). The SuperMAG data processing technique, *Journal of Geophysical Research*, Vol. 117, A09213, DOI: 10.1029/2012JA017683.

Guineva, V., Werner, R., Bojilova, R., Raykova, L., Atanassov, A., Valev, D. (2024a). Analysis of substorms related to strong MPB at Panagyurishte station in 2022, *Proceedings of the Sixteenth Workshop "Solar Influences on the Magnetosphere, Ionosphere and Atmosphere"*, pp. 56–63, DOI: 10.31401/WS.2024.proc.

Guineva, V., Werner, R., Bojilova, R., Raykova, L., Atanassov, A., Valev, D. (2024b). Study of the midlatitude positive bays at the magnetic station Panagyurishte during the descending phase of Solar Cycle 24, *Proceedings of the Twentieth Anniversary International Scientific Conference SES2024*, pp. 48–54.

Guineva, V., Werner, R., Bojilova, R., Raykova, L., Atanassov, A., Valev, D. (2024c). A methodology to estimate the MPB parameters, *Proceedings of the 47th Annual Seminar "Physics of Auroral Phenomena"*, pp. 16–19, DOI: 10.51981/2588-0039.2024.47.003.

Hajra, R., Tsurutani, B.T., Lakhina, G.S., Lu, Q., Du, A. (2024). Interplanetary causes and impacts of the May 2024 superstorm on the geosphere: An overview, *Astrophysical Journal*, Vol. 974, pp. 264–276, DOI: 10.3847/1538-4357/ad7462.

Kleimenova, N.G., Despirak, I.V., Malysheva, L.M., Gromova, L.I., Lubchich, A.A., Roldugin, A.V., Gromov, S.V. (2023). Substorms on a contracted auroral oval, *Journal of Atmospheric and Solar-Terrestrial Physics*, Vol. 245, pp. 106049–106062, DOI: 10.1016/j.jastp.2023.106049.

Kleimenova, N.G., Gromova, L.I., Gromov, S.V., Malysheva, L.M. (2025). Ground-based geomagnetic disturbances and Pi2 pulsations in the main phase of the superstorm on May 10, 2024, *Advances in Space Research*, in press, DOI: 10.1016/j.asr.2025.04.025.

Loewe, C.A., Prolss, G.W. (1997). Classification of mean behavior of magnetic storms, *Journal of Geophysical Research*, Vol. 102, No. A7, pp. 14209–14213, DOI: 10.1029/96JA04020.

Lockwood, M., Owens, M.J., Brown, W., Vázquez, M. (2025). The May 2024 event in the context of auroral activity over the past 375 years, *Monthly Notices of the Royal Astronomical Society*, Vol. 540, No. 4, pp. 3596–3624, DOI: 10.1093/mnras/staf827.

Lubchich, A.A., Despirak, I.V., Werner, R. (2023). Intense mid-latitude magnetic disturbances and solar wind conditions, *Proceedings of the Fifteenth Workshop "Solar Influences on the Magnetosphere, Ionosphere and Atmosphere"*, pp. 61–66, DOI: 10.31401/WS.2023.proc.

McPherron, R.L. (1972). Substorm-related changes in the geomagnetic tail: The growth phase, *Planetary and Space Science*, Vol. 20, No. 9, pp. 1521–1539, DOI: 10.1016/0032-0633(72)90054-2.

McPherron, R.L., Chu, X. (2017). The midlatitude positive bay and the MPB index of substorm activity, *Space Science Reviews*, Vol. 206, pp. 91–122, DOI: 10.1007/s11214-016-0316-6.

Newell, P.T., Gjerloev, J.W. (2011a). Evaluation of SuperMAG auroral electrojet indices as indicators of substorms and auroral power, *Journal of Geophysical Research*, Vol. 116, A12211, DOI: 10.1029/2011JA016779.

Newell, P.T., Gjerloev, J.W. (2011b). Substorm and magnetosphere characteristic scales inferred from the SuperMAG auroral electrojet indices, *Journal of Geophysical Research*, Vol. 116, A12232, DOI: 10.1029/2011JA016936.

Tsurutani, B.T., Hajra, R., Echer, E., Gjerloev, J.W. (2015). Extremely intense (SML ≤ –2500 nT) substorms: Isolated events that are externally triggered?, *Annales Geophysicae*, Vol. 33, No. 5, pp. 519–524, DOI: 10.5194/angeo-33-519-2015.

Wang, R., Ying, D., Liu, Y.D., Zhao, X., Hu, H. (2024). Unveiling key factors in solar eruptions leading to the solar superstorm in May 2024, *Astronomy & Astrophysics*, Vol. 692, A112, DOI: 10.1051/0004-6361/202452008.

Waters, C.L., Anderson, B.J., Liou, K. (2001). Estimation of global field-aligned currents using the Iridium® system magnetometer data, *Geophysical Research Letters*, Vol. 28, pp. 2165–2168, DOI: 10.1029/2000GL012725.

Weiler, E., Möstl, C., Davies, E.E., Veronig, A.M., Amerstorfer, U.V., Amerstorfer, T., Le Louëdec, J., Bauer, M., Lugaz, N., Haberle, V., Rüdisser, H.T., Majumdar, S., Reiss, M. (2025). First observations of a geomagnetic superstorm with a sub-L1 monitor, *Space Weather*, Vol. 23, No. 3, e2024SW004260, DOI: 10.1029/2024SW004260.

Werner, R., Guineva, V., Atanassov, A., Bojilova, R., Raykova, L., Valev, D., Lubchich, A., Despirak, I. (2021). Calculation of the horizontal power perturbations of the Earth surface magnetic field, *Proceedings of the Thirteenth Workshop "Solar Influences on the Magnetosphere, Ionosphere and Atmosphere"*, pp. 159–164, DOI: 10.31401/WS.2021.proc.